Radical Ion States of Platinum Acetylide Oligomers

Thomas Cardolaccia,[†] Alison M. Funston,[‡,||] M. Erkan Kose,[†,§] Julia M. Keller,[†] John R. Miller,*[,‡] and Kirk S. Schanze*[,†]

Department of Chemistry, University of Florida, PO Box 117200, Gainesville, Florida 32611, and Chemistry Department, Brookhaven National Laboratory, Upton, New York 11973

Received: May 15, 2007; In Final Form: July 2, 2007

The ion radicals of two series of platinum acetylide oligomers have been subjected to study by electrochemical and pulse radiolysis/transient absorption methods. One series of oligomers, Pt_n, has the general structure Ph−C≡C−[Pt(PBu$_3$)$_2$−C≡C−(1,4-Ph)−C≡C−]$_n$−Pt(PBu$_3$)$_2$−C≡C−Ph (where $x = 0-4$, Ph = phenyl and 1,4-Ph = 1,4-phenylene). The second series of oligomers, Pt_4T_n, contain a thiophene oligomer core, −C≡C−(2,5-Th)$_n$−C≡C− (where $n = 1-3$ and 2,5-Th = 2,5-thienylene), capped on both ends with −Pt(PBu$_3$)$_2$−C≡C−(1,4-Ph)−C≡C−Pt(PBu$_3$)$_2$−C≡C−Ph segments. Electrochemical studies reveal that all of the oligomers feature reversible or quasi-reversible one-electron oxidation at potentials less than 1 V versus SCE. These oxidations are assigned to the formation of radical cations on the platinum acetylide chains. For the longer oligomers multiple, reversible one-electron waves are observed at potentials less than 1 V, indicating that multiple positive polarons can be produced on the oligomers. Pulse-radiolysis/transient absorption spectroscopy has been used to study the spectra and dynamics of the cation and anion radical states of the oligomers in dichloroethane and tetrahydrofuran solutions, respectively. All of the ion radicals exhibit two allowed absorption bands: one in the visible region and the second in the near-infrared region. The ion radical spectra shift with oligomer length, suggesting that the polarons are delocalized to some extent on the platinum acetylide chains. Analysis of the electrochemical and pulse radiolysis data combined with the density functional theory calculations on model ion radicals provides insight into the electronic structure of the positive and negative ion radical states of the oligomers. A key conclusion of the work is that the polaron states are concentrated on relatively short oligomer segments.

Introduction

Platinum acetylide polymers and oligomers are of interest for possible use in optical and optoelectronic applications.[1−5] On a more fundamental level, platinum acetylide conjugated materials provide a unique platform for investigation of π conjugation mediated by metal dπ/carbon pπ interactions.[6−12] We recently reported photophysical studies of a series of monodisperse platinum acetylide oligomers of the type, −[*trans*-Pt(PBu$_3$)$_2$−C≡C−Ph−C≡C−]$_n$, where Ph = 1,4-phenylene.[11,13] This investigation provides evidence that in the first singlet excited state ($^1\pi,\pi^*$) the exciton is delocalized over a chromophore consisting of five or more repeat units. Interestingly, in the first triplet excited state ($^3\pi,\pi^*$) the exciton is considerably more confined; optical spectroscopy and density functional theory (DFT) calculations support a model in which the triplet is restricted to a chromophore consisting of the −[Pt(PBu$_3$)$_2$−C≡C−Ph−C≡C−Pt(PBu$_3$)$_2$]− unit.[6,8,10,13] Experimental results and DFT calculations also suggest that delocalization in the platinum acetylide systems is strongly influenced by the relative conformation of the phenylene rings and the square planar PtP_2C_2 units along the oligomer backbone.[13]

In continuation of our investigation of π conjugation in platinum acetylide systems, we recently carried out a series of electrochemical and pulse-radiolysis studies on an extended series of platinum acetylide oligomers. In particular, this work has examined the electrochemistry and optical spectra of the anion and cation radicals of the series of oligomers Pt_n (Scheme 1, $n = 1-5$), which have previously been the subject of optical spectroscopy studies.[11,13] This series contains a regular repeat unit structure in the backbone consisting of the square planar $Pt^{II}(PBu_3)_2C_2$ unit alternating with 1,4-phenylene ethynylene. In addition, the new series of oligomers Pt_4T_n (Scheme 1, $n = 1-3$) was also examined. The Pt_4T_n oligomers each contain four $Pt^{II}(PBu_3)_2C_2$ centers; however, the "core" organic π-system consists of a thiophene oligomer segment containing one, two, or three 2,5-thienylene units. The electrochemical and pulse-radiolysis studies give insight into the spectroscopy, electronic structure, and delocalization in the ion-radical states of the oligomers. The properties of the ion-radical states of these oligomers are of fundamental interest, as they provide information concerning the influence of the metal centers in mediating π conjugation in organometallic oligomers.

The methods we have used in the present study[14−19] and other time-of-flight techniques[20−24] have been successfully used to study charge transport and delocalization in organic conjugated oligomers and polymers. In particular, thiophene-based oligomers[25,26] and polymers[27,28] have received considerable attention due to their promising optical, electrochemical, and electronic properties. Examples of organometallic systems are less common but are gaining increasing attention.[29−41] The results of the

* To whom correspondence should be addressed. E-mail: kschanze@chem.ufl.edu (K.S.S.), jrmiller@bnl.gov (J.R.M.).
† University of Florida.
‡ Brookhaven National Laboratory.
§ Current Address: National Renewable Energy Laboratory, 1617 Cole Blvd, Golden, CO 80401.
|| Current Address: School of Chemistry and Bio21 Institute, The University of Melbourne, Victoria, 3010, Australia.

10.1021/jp0737552 CCC: $37.00
Published on Web 08/24/2007

SCHEME 1

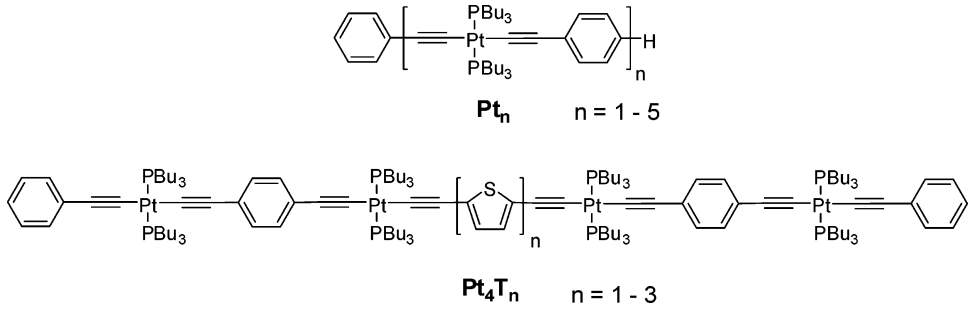

present investigation demonstrate that in the Pt_n series there is some delocalization in the ion radicals; however, the results do suggest that the polarons are concentrated onto a comparatively short oligomer segment. The results on the Pt_4T_n series indicate that in both the cation and anion radicals the charge carriers are concentrated near and on the thiophene segments in the core of the oligomers.

Experimental Section

Synthesis. The synthesis of oligomers Pt_1-Pt_5 was described previously.[11] The synthesis and characterization of the Pt_4T_n oligomers are described in detail in the Supporting Information.[42]

Electrochemistry. Electrochemical measurements were performed using a BAS CV-50W voltammetric analyzer (Bioanalytical Systems, Inc., www.bioanalytical.com) in dry methylene chloride solutions containing 0.1 M tetra-*n*-butylammonium hexafluorophosphate (TBAH, Aldrich) as the supporting electrolyte and with a three-electrode setup consisting of a platinum microdisk (2 mm^2) working electrode, a platinum wire auxiliary electrode, and a silver wire quasi-reference electrode. Solutions were degassed by bubbling with argon prior to measurements, and a positive pressure of argon was maintained during the measurements. The concentrations of oligomers in the solutions were all in the 10 μM range. Cyclic voltammetry was performed with a scan rate of 100 mV s^{-1}. Differential pulse voltammetry was performed with a scan rate of 4 mV s^{-1}, a pulse amplitude of 50 mV, and pulse width of 50 ms. All potentials were calibrated against the ferrocene/ferricinium couple added as an internal standard, and the potentials listed herein are converted to the SCE reference using a value of $E(Fc^+/Fc) = 0.43$ V versus SCE in methylene chloride.[29]

Pulse Radiolysis. This work was carried out at the Brookhaven National Laboratory Laser-Electron Accelerator Facility (LEAF). The LEAF facility and the methods used are described elsewhere.[43,44] The electron pulse ($\leq$120 ps duration) was focused into a quartz cell with an optical path length of 20 mm containing the solution of interest. The monitoring light source was a 75 W Osram xenon arc lamp pulsed to a few hundred times its normal intensity. Wavelengths were selected using either 40 or 10 nm bandpass interference filters. Transient absorption signals were detected with either FND-100Q silicon ($\leq$1000 nm) or GAP-500L InGaAs ($\geq$1100 nm) diodes and digitized with a Tektronix TDS-680B oscilloscope. The transmission/time data were analyzed, and reaction rate constants were determined in a scheme that accounts for geminate and homogeneous recombination.[45] The model was fit to the data using nonlinear least-squares fitting in Igor Pro software (Wavemetrics). Where not stated, uncertainties are 15%. Molar extinction coefficients of the radical cations were calculated using $G(DCE^{\bullet+}) = 0.68$,[46] where G is the radiation chemical yield (molecules produced/100 eV). The reported G values for the electron in THF varied greatly, and $G(e^-_{THF}) = 0.60$,[47-50] the average of a number of reported values, was used to calculate the anion extinction coefficients.

The total dose per pulse was determined before each series of experiments by measuring the change in absorbance of the electron in water. The dose received was calculated using ϵ-(700 nm, e^-_{aq}) = 18 830 M^{-1} cm^{-1} and $G(e^-_{aq}) = 2.97$. The dose was corrected for the difference in electron density of the organic solvents used compared to that of water. Radiolytic doses of 5−18 Gy were employed. For the 1,2-dichloroethane (DCE) solutions, dissolved oxygen was removed by purging with argon gas for at least 10 min, and the cells were then sealed with septa and Parafilm. Solutions in THF were prepared in an argon environment and sealed under argon with Teflon vacuum stoppers. Samples were prepared immediately prior to use. During irradiation, samples were exposed to as little UV light as possible to avoid photodecomposition, although no evidence of this occurring was found within the time frames monitored. Measurements were carried out at 21 °C.

Calculations. Quantum chemical calculations were carried out using the Gaussian 03 program.[51] The geometries of the Pt_2 cation and anion were optimized using the B3LYP hybrid functional within C_{2h} symmetry. The SDD basis set was used to employ the Stuttgart/Dresden relativistic effective core potential for explicit treatment of platinum electrons, and the 6-31g(d,p) was used for the rest of the atoms in the molecules. Time-dependent density functional theory calculations were performed employing the same basis sets and methods used for geometry optimizations for both the cation and anion. The butyl groups attached to the phosphorus atoms were truncated to methyl groups to decrease the computational time.

Results

Electrochemistry. Oxidation and reduction of the Pt_n and Pt_4T_n oligomers were explored using cyclic voltammetry and differential pulse voltammetry (DPV) techniques. Measurements were carried out in argon outgassed methylene chloride with TBAH (0.1 M) as the supporting electrolyte. For all of the oligomers, cathodic sweeps produced only irreversible waves for reduction in the range −1.0 to −1.3 V. This data will not be discussed here. However, for all of the oligomers, anodic sweeps revealed one or more reversible (or quasi-reversible) waves for oxidation of the complexes in the range from +0.6 to +1.1 V. The half-wave values for the observed waves are listed in Table 1, and Figures 1 and 2 illustrate the anodic DPV sweeps for the Pt_n and Pt_4T_n series, respectively (the cyclic voltamograms are provided in Figures S1 and S2).

First, we consider the anodic electrochemical data for the Pt_n series, where revealing trends are seen. The shortest oligomers, Pt_1 and Pt_2, exhibit only a single anodic wave at +1.11 and +0.89 V, respectively (the observation for Pt_1 is consistent with a previous electrochemical study of the same complex).[52] Sweeps to more positive potentials do not reveal any additional

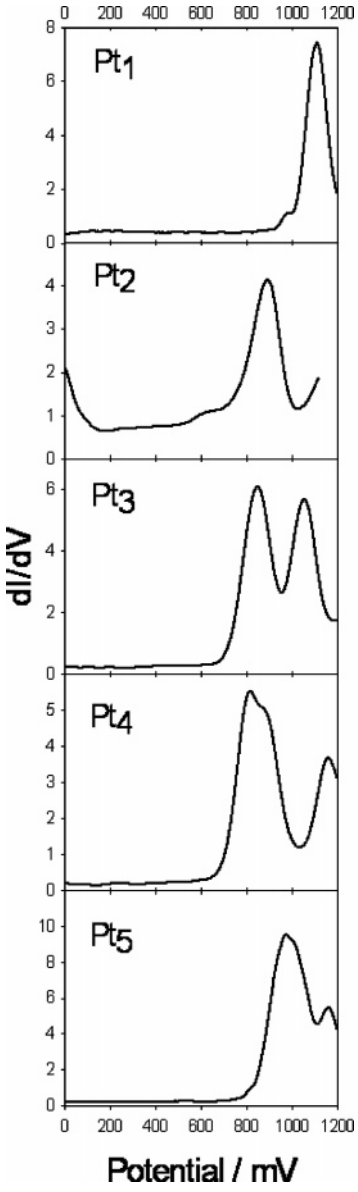

Figure 1. Differential pulse voltammograms for Pt_n oligomers in CH_2Cl_2/0.1 M TBAH.

TABLE 1: Redox Potentials (V vs SCE) for Pt_n and Pt_4T_x Oligomers[a]

oligomer	$E_{1,red}$	$E_{1,ox}$	$E_{2,ox}$	$E_{3,ox}$
Pt_1	−1.29[b]	1.11[b]		
Pt_2	−1.27[b]	0.89[b]		
Pt_3	−1.19	0.85	1.06	
Pt_4	−1.30	0.81	0.88	
Pt_5	−1.29	0.98[b]	1.16[b]	
Pt_4T_1	−1.08[b]	0.71	1.09 (2 e$^-$)	
Pt_4T_2	−1.02[b]	0.63	1.01 (2 e$^-$)	
Pt_4T_3	−1.01	0.64	0.88	1.08

[a] Argon outgassed CH_2Cl_2/0.1 M TBAH. [b] Irreversible wave.

reversible waves, indicating that for the shortest oligomers only the cation radicals ($Pt_n^{\bullet+}$) are stable on the electrochemical time-scale. Interestingly, the longer oligomers reveal two reversible anodic waves. In particular, Pt_3 features two clearly resolved waves at +0.85 and +1.06 V, whereas in Pt_4 two very closely spaced waves are observed with peak potentials at +0.81 and +0.88 V. The longest oligomer studied, Pt_5, only exhibits a single wave at +0.98 V; because this wave is quasi-reversible (see cyclic voltammogram in Figure S1), it is not possible to confirm whether it is a one- or two-electron wave.[53] Taken

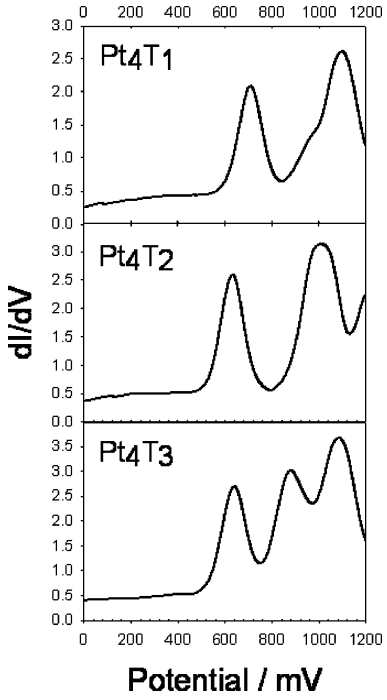

Figure 2. Differential pulse voltammograms for Pt_4Th_n oligomers in CH_2Cl_2/0.1 M TBAH.

together, the anodic electrochemical results on the Pt_n series suggest that in Pt_3 and Pt_4 (and possibly in Pt_5) both the mono- and dication (i.e., Pt_n^{2+}) states are stable on the electrochemical time-scale. The fact that the difference in the potentials for the successive oxidation waves decreases with oligomer length strongly suggests that oxidation produces polaron states that are concentrated on a short oligomer segment, which interact moderately in Pt_3 (ΔE = 210 mV) and only weakly in Pt_4 (ΔE = 70 mV). This issue will be explored more thoroughly in the discussion section below.

The anodic electrochemistry of the Pt_4T_n series clearly shows that the first oxidation produces polaron states that are concentrated near the thienylene core of the oligomers. In particular, all three of the Pt_4T_n oligomers feature a nicely reversible one-electron wave in the range +0.6 to +0.7 V. This oxidation is clearly associated with the thienylene core of the oligomers, as it occurs at a considerably less positive potential than the first oxidation of the Pt_n oligomers which lack a thienylene segment. In Pt_4T_1 and Pt_4T_2, this first wave is followed by a broad, reversible 2e$^-$ wave. For Pt_4T_1, the second 2e$^-$ wave is likely due to oxidations centered on the two "peripheral" −[Pt-$(PBu_3)_2$−C≡C−Ph−C≡C−] segments of the oligomer, whereas in Pt_4T_2, the second wave is believed to arise due to a second oxidation of the bithiophene core segment and an oxidation centered on the peripheral segment of the oligomers. For Pt_4T_3, three separate 1e$^-$ waves are observed; the first two waves are assigned to one- and two-electron oxidation of the terthiophene core oligomer while the third wave is believed to be due to oxidation of a peripheral −[Pt$(PBu_3)_2$−C≡C−Ph−C≡C−] segment.[54]

Pulse Radiolysis Ion Radical Spectra. Ion radicals were generated by pulse radiolysis at Brookhaven National Laboratory.[43,44] The $Pt_n^{\bullet-}$ spectra in THF were measured at 15 ns and $Pt_n^{\bullet+}$ spectra in DCE were measured at 300 ns; the later time in DCE was due to the slower growth.

Cation Radicals. First, we discuss the cation radical spectra shown in Figure 3a for the Pt_n series. All of the oligomer cation radicals feature an intense absorption band in the visible ($\epsilon \approx$

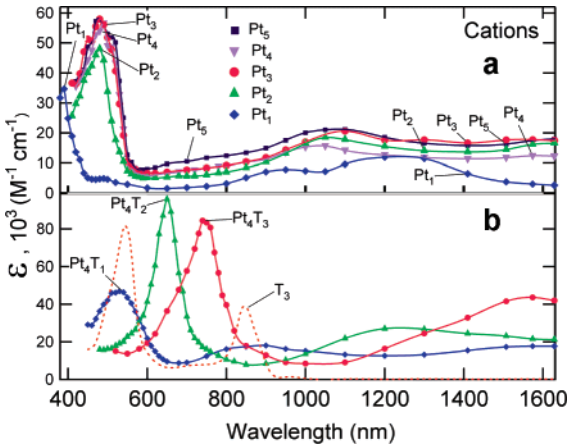

Figure 3. Transient absorption spectra for radical cations of (a) Pt_n and (b) Pt_4T_n in DCE. The spectrum of terthiophene (T_3) cation is shown for comparison.

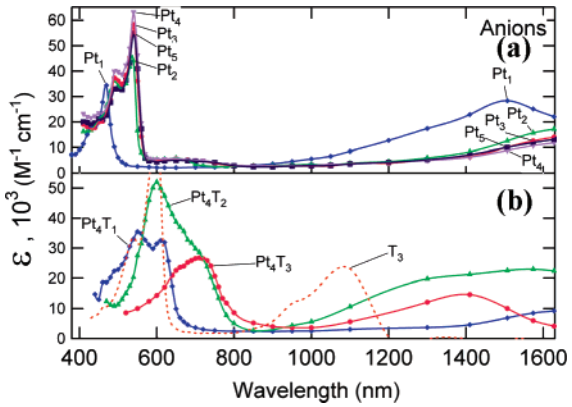

Figure 4. Transient absorption spectra for radical anions of (a) Pt_n and (b) Pt_4T_n in THF. The spectrum of terthiophene (T_3) anion is shown for comparison.

5×10^4 M^{-1} cm^{-1}) and a weaker absorption in the near-IR range. For the visible band, the absorption maximum shifts significantly between Pt_1 and Pt_2. There is a slight red shift in going from Pt_2 to Pt_3, and then the band maximum remains almost the same for Pt_3, Pt_4, and Pt_5. The same trend is observed for the near-IR band, where the absorption maximum red shifts significantly between Pt_1 and Pt_2, but then there is little shift beyond Pt_2. These results suggest a rather localized cation radical species, consistent with the electrochemistry data.

In Figure 3b, the spectra of the Pt_4T_n radical cations are shown. These spectra also exhibit two absorption bands, one in the visible and the second in the near-IR. Both of the bands red shift significantly across the series suggesting that in the cations polarons become more delocalized as the length of the thiophene segment increases. The strong effect of the T_n on the spectra suggests that the radical cation is concentrated near or on the oligo(thiophene) segment of the oligomers, as the visible bands are very red shifted compared to visible absorption bands observed in the Pt_n series.

Anion Radicals. We will again first look at the anion radical spectra of the Pt_n oligomer series displayed in Figure 4a. Again, there are two bands observed in the spectra: one in the visible and one extending well into the IR region (except Pt_1). But the data suggests the presence of an anion radical that is concentrated on a short oligomer segment, as the maximum of absorption of both bands changes considerably between Pt_1 and Pt_2 but then changes little up to Pt_5. The spectra of the radical anions of the Pt_4T_n series shown in Figure 4b also feature the

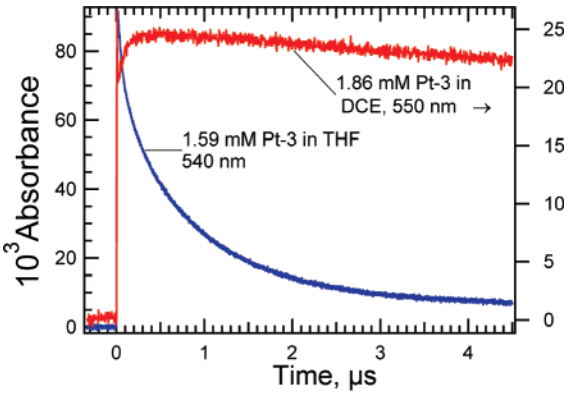

Figure 5. Transient absorption as a function of time for Pt_3 anions and cations near λ_{max}.

TABLE 2: Rate Constants for Attachment of Solvated Electrons in THF or Holes in DCE to Pt_n Oligomers

n	$k(e^-s)/M^{-1}$ s^{-1}	$k(DCE^+)/M^{-1}$ s^{-1}
1	9.8×10^{10}	1.5×10^{10}
2	1.7×10^{11}	2.4×10^{10}
3	2.1×10^{11}	2.5×10^{10}
4	2.5×10^{11}	3.3×10^{10}
5	3.2×10^{11}	3.7×10^{10}

two bands seen in the Pt_n series. The visible region bands follow the same trend observed in the radical cation spectra with a red shift from Pt_4T_1 to Pt_4T_3. The low-energy band displayed by these radical anions shows a surprising inverse trend. Whereas it is around 1400 nm for Pt_4T_3, it seems to red shift to 1600 nm for Pt_4T_2 and extends well beyond 1600 nm in Pt_4T_1.

Charge Attachment Rates and Ion Recombination. Rate constants for attachment to Pt_n of solvated electrons (e^-_s) in THF or positive charge from $DCE^{\bullet+}$ in DCE are given in Table 2. Decay of e^-s or $DCE^{\bullet+}$ in the neat solvents, principally due to recombination of geminate ion, was accounted for in determination of the rate constants. The rate constants for the Pt_n radical anions were obtained from the decay of e^-_s. The rate constants for the radical cations were obtained from the growth of the Pt_n radical cations because strong absorbance of those ions made measurement of $DCE^{\bullet+}$ difficult. The rate constants are faster in THF due to the high mobility of e^-_s. In both cases, the rate constants are linear in n for the $n = 1-5$ oligomers; plots of rate versus n are shown in Figure S3. The intercepts are not zero, as expected, because the Pt_1 oligomer is longer than the increment in size between successive oligomers. The approximate linearity with n may be slightly surprising because diffusion controlled attachment reactions to long molecules become nonlinear in n;[15,55–58] these effects may not be pronounced in the relatively short oligomers in the present study.

Production of radical anions and cations is accompanied by production of counterions. The rate constants for reaction of counterions with the formed Pt_n radical cations or anions are accelerated to $\sim 2 \times 10^{11}$ M^{-1} s^{-1} by the Coulomb attraction of the opposite charges. In THF, each accelerator pulse produces ~ 1 μM anions and an identical concentration of positive ions, so the rate of ion recombination in the first half-life is $\sim 10^{11} \times 10^{-6} = 10^5$ s^{-1}. In THF, (RH) radical cations are thought to decompose to radicals and solvated protons, $RH^{\bullet+} + RH \rightarrow R^{\bullet} + RH_2^+$. In DCE, (RCl) electrons attach dissociatively, $e^- + RCl \rightarrow R^{\bullet} + Cl^-$, and recombination with those Cl^- ions is expected to proceed with kinetics similar to those in THF. Thus, over a few microseconds, the radical cations in DCE are expected to combine with Cl^- ions and the radical anions in

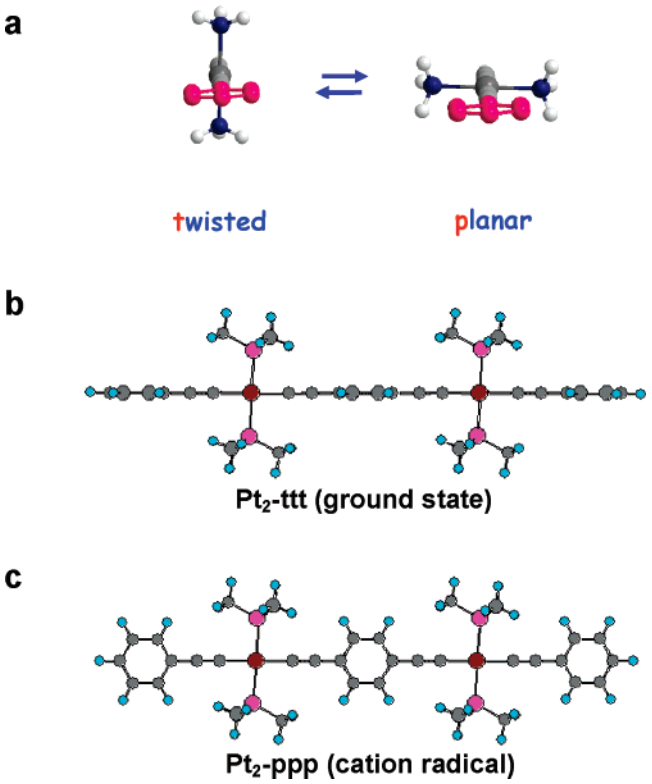

Figure 6. (a) Schematic illustration of two limiting conformations for the oligomers, twisted (t) and planar (p). (b) Energy minimized conformation of ground state Pt_2. (c) Energy minimized conformation of $Pt_2^{\bullet+}$.

THF are expected to combine with solvated protons, RH_2^+. Figure 5 shows that little decay occurs for $Pt_3^{\bullet+}$; upon combination with Cl^- the cations remain as stable ion pairs ($Pt_3^{\bullet+}$,Cl^-), which have similar absorption to that of free $Pt_3^{\bullet+}$. By contrast, in THF substantial decay of $Pt_3^{\bullet-}$ is seen. Apparently, upon combination with RH_2^+ a proton is transferred to $Pt_3^{\bullet-}$. Absorption spectra (Figure S4) show that the sharp band of $Pt_3^{\bullet-}$ at 540 nm disappears almost completely in ~5 μs. Some broad absorption still remains in the near-IR region. The other oligomers behave similarly. The spectra at long times, tentatively identified as the H-atom adduct of $Pt_3H^{\bullet}$, apparently contain some features similar to those of $Pt_3^{\bullet-}$, but impurities could have contributed to the decay of $Pt_3^{\bullet-}$. Therefore the identity of the product is not established unambiguously.

Density Functional Theory Calculations. Quantum chemical calculations were carried out using Pt_2 as a model in order to provide insight into the electronic structure and geometry of the ion radicals produced by one electron oxidation and reduction. These calculations were done using density functional theory (DFT) within the Gaussian 03 program. (Calculations on the longer oligomers were not done due to the significant amount of computational time required.) The computational methods used in the present work were the same as those used in a recently reported study, where we examined the electronic structure and geometry of the ground and excited states of Pt_2, Pt_3, and Pt_4.[13,59] A point that was explored carefully in our previous investigation is the effect of rotation of the phenylene units on the energy of the Pt_2 ground state (i.e., the "t" and "p" conformers, see Figure 6a).[13] This study showed that in the ground state the lowest energy conformation (the global energy minimum) is that shown in Figure 6b. This conformer is referred to as Pt_2-ttt, where the t's signify that each of the three phenylene units is oriented perpendicular relative to the plane defined by the square-planar *trans*-$Pt(PBu_3)_2(C)_2$ units. The previous study also revealed that in the ground state the barrier to rotation of the phenylene units around the molecular axis is low (<1 kcal mol^{-1}) and therefore conformers in which one or more phenylenes are in the "p" conformation are populated at ambient temperature.[60]

TABLE 3: TDDFT Results for Cation and Anion States of Pt_2

structure	wavelength/nm	transitions	oscillator strength
$Pt_2^{+\bullet}$	429	171B→87B (80%)	0.3973
	451	187A→188A (42%)	0.6613
		171B→187B (13%)	
	1575	186B→187B (97%)	1.0403
$Pt_2^{-\bullet}$	483	187B→188B (73%)	0.7353
	1953	188A→189A (98%)	0.9768

The DFT geometry optimized structure of the radical cation of Pt_2 ($Pt_2^{\bullet+}$) is shown in Figure 6c. Interestingly, in the cation state, the oligomer exhibits a distinct change in the lowest energy geometry compared to that of the ground state neutral. Specifically, in the cation, the lowest energy conformer is ppp (all of the phenylenes are in plane) and the DFT results show that for the radical cation the ttt conformer is 2.4 kcal mol^{-1} higher in energy relative to ppp. A similar result is obtained for the anion radical ($Pt_2^{\bullet-}$). The lowest energy conformation of this species is also ppp (Figure 6c), and DFT results show that in the anion the ttt conformer is ≈15 kcal mol^{-1} higher than ppp. This result implies that the barrier to rotation of the phenylene units is considerably higher in the anion state.

More insight into the structure of the cation and anion states of Pt_2 comes from Figure 7 which illustrates the difference in bond lengths for the DFT geometry optimized $Pt_2^{\bullet+}$ and $Pt_2^{\bullet-}$ structures compared to the neutral ground state structure. First, for the cation state (Figure 7, red bars), the geometry distortion is concentrated in the center of the oligomer, that is, on the structural unit [—$Pt(P)_2$—C≡C—Ph—C≡C—$Pt(P)_2$—]. Interestingly, there is also a clear lengthening of the Pt—P bonds and shortening of the Pt_7—C_9 (and Pt_{17}—C_{16}) bond. Both of these features result from a decrease in electron density at Pt, which decreases dπ(Pt) → P back bonding and increases the C—Pt π bonding. For the anion state, the geometric distortion is somewhat more evenly spread out across the oligomer and yet there exists some concentration in the [—$Pt(P)_2$—C≡C—Ph—C≡C—$Pt(P)_2$—] core. Note that in the anion there is a considerable *shortening* of the Pt—P bond, consistent with an increased charge density at Pt and a consequent increased dπ(Pt) → P back-bonding interaction.

The DFT calculations imply that in the cation and anion states of Pt_2 there is some concentration of the polaron in the [—$Pt(P)_2$—C≡C—Ph—C≡C—$Pt(P)_2$—] unit, a point also supported by the computed atomic Mullikan charges (see Figure S5). The difference charges upon creating a cation are largest on the two Pt atoms in $Pt_2^{\bullet+}$ (or $Pt_2^{\bullet-}$) and show a tendency to decrease for atoms farther from the Pt atoms. The lowest energy conformation for the polaron states is clearly ppp, which is in contrast to the ground state, and has a slight energetic preference for the ttt conformation. These differences in geometry between the neutral and charged states may provide the basis for concentration of the polaron onto a relatively short segment, even in the longer oligomers.

Time-dependent DFT (TDDFT) calculations were also performed on $Pt_2^{\bullet+}$ and $Pt_2^{\bullet-}$ in order to provide insight into the optical transitions that are experimentally observed for the ion radicals. The transitions were computed using the energy

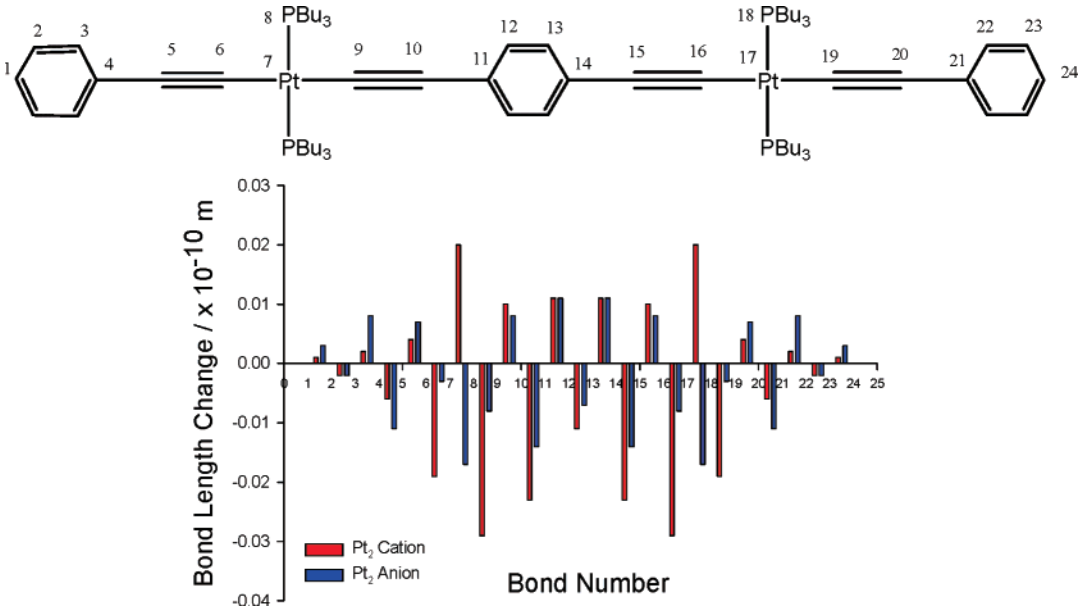

Figure 7. Plot showing computed bond length differences for $Pt_2^{\bullet+}$ and $Pt_2^{\bullet-}$ relative to the neutral (Pt_2). The structure shown at the top indicates the atomic numbering used in the graph.

minimum (ppp) conformations for both $Pt_2^{\bullet+}$ and $Pt_2^{\bullet-}$. Table 3 provides a summary of the TDDFT results in terms of the wavelength maxima for the transitions with significant oscillator strength along with the orbital transitions that make significant contributions to the CI. Simulated spectra are shown in Figure S6. As can be seen, the computed spectra are in excellent agreement with the experimental spectra. In particular, for the cation ($Pt_2^{\bullet+}$) the experimental spectrum shows a broad band in the visible region with $\lambda_{max} \approx 480$ nm along with very broad near-infrared transitions with $\lambda_{max} \approx 1050$ and 1700 nm. This compares with the simulated spectrum that exhibits bands at $\lambda = 429$ and 451 nm in the visible region and $\lambda = 1575$ nm in the near-infrared region. For the anion ($Pt_2^{\bullet-}$), the experimental spectrum shows a narrow band in the visible region with $\lambda = 535$ nm and a near-infrared band at $\lambda > 1600$ nm. The TDDFT computed spectrum is in good agreement with bands at $\lambda = 483$ and 1953 nm.

The TDDFT calculations also provide insight concerning the molecular orbitals involved in the visible and near-infrared transitions for the ion radicals. Figure 8 shows a schematic illustration of the qualitative molecular orbital diagrams for the neutral, cation, and anion; the dominant transitions that contribute to the visible and near-infrared absorptions for each species are labeled on the scheme. The important feature with respect to this diagram is that it is very similar to that of the ion radicals of organic conjugated oligomers such as oligo(thiophene)s and oligo(phenylene vinylene)s.[61,62] In particular, for the radical cation, the visible and near-infrared transitions are dominated by the SOMO−(SOMO+1) and (SOMO−1)−SOMO transitions, respectively. For the anion radical, the visible and near-infrared transitions are dominated by the (SOMO−1)−SOMO and SOMO−(SOMO+1) transitions, respectively. This result suggests that the structure of the polaron states in the platinum acetylide oligomers is qualitatively similar to those for organic π-conjugated systems. In addition, we conclude that (intervalence) charge-transfer transitions do not contribute significantly to the visible or infrared transitions.[63]

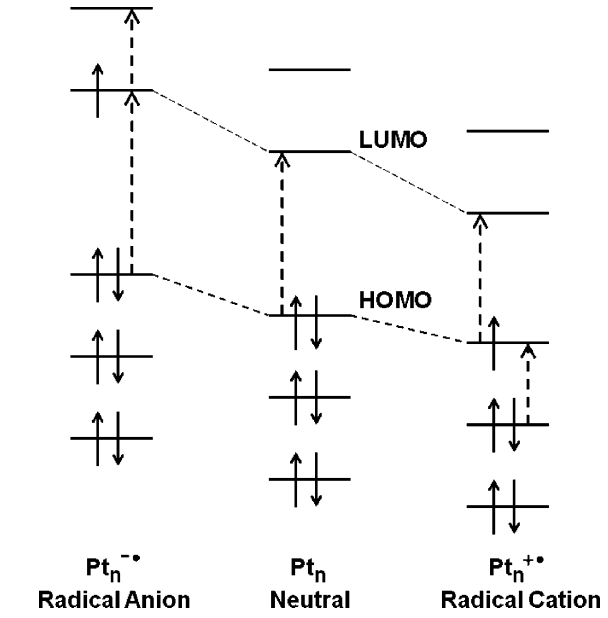

Figure 8. Frontier molecular orbital levels and allowed transitions (dashed lines) of the platinum acetylide neutrals (Pt_n), radical cations ($Pt_n^{\bullet+}$), and radical anions ($Pt_n^{\bullet-}$).

Discussion

Polaron States in Conjugated Oligomers and Polymers. The growing importance of conjugated organic molecules and polymers as the active materials in electronic and optoelectronic devices has stimulated a number of fundamental studies that have explored the nature of the charged (polaron) states of oligomer model systems.[16,61,62,64−75] These studies have examined oligomers of thiophene (OTh), phenylene vinylene (OPV), phenylene, or fluorene, and some work has been done on mixed organic−organometallic conjugated oligomers.[30,33,34,37,76] This work has provided insight concerning the electronic and geometric structure of the polaron states in π-conjugated systems. In particular, studies of the optical spectra and electrochemistry of OThs of varying length suggest that the spatial extent of the positive polaron is approximately five thienylene repeat units[61] or ∼2 nm. Similar studies of OPV radical cations suggest that the positive polaron is delocalized over approximately six to eight phenylene vinylene repeats[62] or ∼4.7 nm. Experimental and theoretical studies of of the

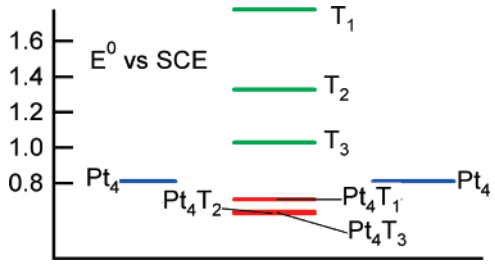

Figure 9. Energy level diagram for energies of Pt_4T_n radical cations based on their redox potentials and those of separate Pt_4 (Table 1) and thiophene oligomers. (Data for the thiophene oligomers (corrected to SCE) is from ref 81.)

positive polaron states of OThs and OPVs reveal a similar pattern.[61,62,77,78] Two optical transitions are observed, one in the near-infrared (P1) and a second in the visible region (P2). In a one-electron approximation, these transitions arise from dipole-allowed excitations from the singly occupied (SOMO) level to the SUMO+1 (P2) and from the highest doubly occupied level (SOMO−1) to the SOMO (P1). Further oxidation of the radical cation state of short OThs affords the doubly oxidized species, which exists as a bipolaron that has a singlet spin multiplicity (i.e., the two unpaired spins combine). In sufficiently long oligomers or polymers, two separate polarons are more stable than the bipolaron.[61,79]

Less information is available on the negative polaron states (anion radicals) of conjugated oligomers. Polyfluorene anions were found to be delocalized over four-and-a-half repeat units or 3.8 nm, and polarons were more stable than bipolarons.[58] Some optical spectra are available for the negative polaron states of OThs and OPVs, and these spectra are qualitatively similar to those of the positive polaron states; that is, they exhibit two bands, one in the visible and the second in the near-infrared regions.[64,69,80] These two transitions arise from dipole-allowed excitations from the lowest doubly occupied level (SOMO−1) to SOMO (visible) and SOMO to (SOMO+1) (near-infrared).

Ion Radical States in Pt_n Oligomers. As noted above, Pt_2, Pt_3, and Pt_4 display one or two quasi-reversible anodic waves arising from oxidation of the oligomers. Analysis of the voltammetric behavior for Pt_2, Pt_3, and Pt_4 suggests that for $n > 2$ it is possible to oxidize an oligomer sequentially through the monocation and dication states. Furthermore, the difference in potentials for the sequential oxidation processes decreases from Pt_3 to Pt_4, and in the latter the difference in the first and second oxidation potentials is ≈80 mV. This behavior implies that one-electron oxidation of the oligomers affords a positive polaron state that is concentrated on a relatively short oligomer segment, and if the oligomer length is >2, it is possible to oxidize the oligomer such that two polarons exist on a single chain. Given that the difference in the oxidation waves is small in Pt_4, this suggests that in this oligomer the two polaron states are sufficiently localized such that they do not interact strongly.

The fact that the positive polaron state is relatively concentrated on the platinum acetylide chain is also supported by the optical absorption data. As shown in Figure 3, the spectra of the $Pt_n^{\bullet+}$ series converge for $n > 2$ in the visible and near-infrared regions. But it should be noted that, with the possible exception of $Pt_1^{\bullet+}$, low-energy onsets of the near-infrared bands are not observed. It is possible that more distinct differences might be seen there, for example, between $Pt_2^{\bullet+}$ and the longer oligomers. The enhanced reversibility seen in the cyclic voltamagram (Figure S1) for Pt_3 relative to that of Pt_2 indicates that $Pt_3^{\bullet+}$ is more stable, supporting a polaron length greater than two units. This behavior contrasts with that seen in the optical spectra of OTh and OPV radical cations, where the visible and near-infrared bands continue to red shift for oligomers with five or more repeat units.[61,62,77,78]

On the basis of these results, we suggest the model shown in Scheme 2 for the structure of the mono- and dication states of Pt_4, which is a model for a longer oligomer. This model implies that the positive polaron in the platinum acetylide chain is concentrated on just over two repeat units as highlighted in blue in Scheme 2. Given the length per repeat unit (ca. 1.0 nm), the length of the polaron is ∼2.2 nm, which is shorter than the lengths of polarons in OPV oligomers or polyfluorene and comparable to estimated lengths of polarons in oligothiophenes. We note that the blue-shaded region in Scheme 2 describes the minimum length of the polaron that is consistent with experimental observations; it could be slightly longer. Moreover, the model suggests that multiple polarons can exist on a single chain in relatively close proximity[61] and that the bipolaron state is not favored over the two separate polarons. The spatial concentration of the polaron that is suggested by this scheme may be driven by several factors including the distortion in geometry (phenylene conformation and bond length changes) as well as the fact that the electronic coupling (π delocalization) through the platinum centers is not as efficient as through a single (or even several) π-conjugated carbon(s). Indeed with respect to this latter point, a recent study of intervalence transfer in a complex of the type, donor—C≡C—$Pt(PR_3)_2$—C≡C—donor$^{\bullet+}$, indicated that electronic coupling through the platinum acetylide center was less efficient compared to a 1,4-linked phenylene (benzene) spacer, thus, leading to the conclusion that platinum transmits electronic coupling but not as effectively as a benzene ring.[63]

Unfortunately, little useful information was obtained from reductive electrochemistry of any of the oligomers. However, the optical spectra of the anion radicals for the Pt_n series provide

SCHEME 2

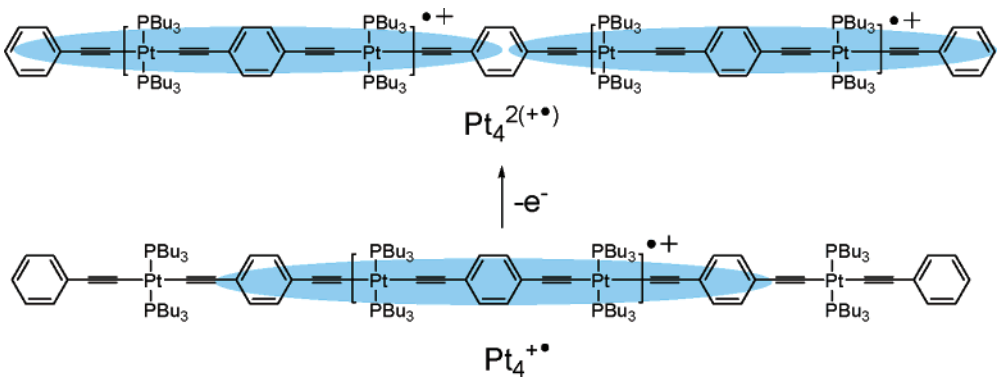

SCHEME 3

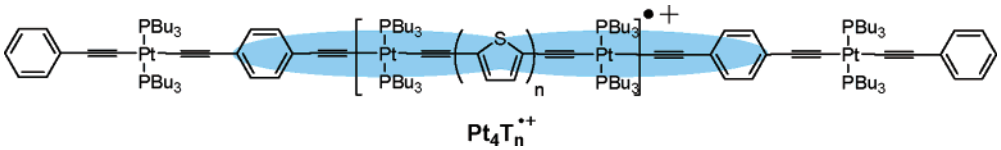

compelling evidence that the negative polaron state is also spatially confined on the chain. Specifically, as shown in Figure 4b, the spectra of the $Pt_n^{\bullet-}$ series are essentially the same in the visible and near-infrared regions for $n \geq 2$. On the basis of this result, we postulate that the negative polaron is concentrated on a single [—$Pt(P)_2$—C≡C—Ph—C≡C—$Pt(P)_2$—] structural unit.

Despite the evidence that suggests the polaron states in the platinum acetylides to be concentrated on relatively short segments, it is interesting that the nature of the dominant optical transitions observed in the visible and near-infared regions is remarkably similar to that of the organic π-conjugated chains. This finding underscores the fact that despite the presence of the heavy metal in the conjugated chain, the electronic structure of the π-electron system is very similar to that of a π-delocalized electron system comprised entirely of light atoms (e.g., B, C, N, O, and/or S), although delocalization lengths appear somewhat shorter. Importantly, there does not appear to be any significant degree of charge-transfer contribution (i.e., metal-to-ligand, ligand-to-metal, or ligand-to-ligand) to the optical transitions observed in the visible or near-infrared regions for the positive and negative polaron states.

Ion Radical States in Pt_4T_n Oligomers. The oxidative electrochemistry of the Pt_4T_n oligomers is distinctly different from that of the Pt_n series. In particular, each Pt_4T_n oligomer exhibits a first oxidation wave that is at a less positive potential relative to that of Pt_4. In addition, the first oxidation wave is at a less positive potential in Pt_4T_2 and Pt_4T_3 relative to Pt_4T_1. (The reader is referred to Figure 9 for a graphical comparison of the oxidation potentials discussed here.) On the basis of these observations, one might infer that the positive polaron in the Pt_4T_n oligomers is concentrated on the thiophene segment. However, it is important to point out that the potential for the first oxidation in each of the Pt_4T_n oligomers occurs at a significantly lower potential compared to OThs of comparable length. Meerholz[81] reported that T_1, T_2, and T_3 are oxidized at 1.78, 1.33, and 1.03 V versus SCE (corrected from Ag/AgCl), respectively, and Baüerle and co-workers reported that the first reversible oxidation for a series of alkyl end-capped OThs occurs at +0.81, +0.75, and +0.69 V versus SCE for $n = 3$, 4, and 5, respectively.[82] Thus, the first oxidation potential of Pt_4T_2 and Pt_4T_3 occurs at a less positive potential than that of a thiophene oligomer with *five* rings. This comparison indicates that the polaron state in ($Pt_4T_n^{\bullet+}$) is stabilized by delocalization into the platinum acetylide units which are on either end of the thiophene oligomer segments.

The optical spectra for the $Pt_4T_n^{\bullet+}$ series also support the notion that the polaron is concentrated near to and on the oligothiophene segment. In particular, the $Pt_4T_n^{\bullet+}$ spectra are characterized by a strong visible absorption band that is red shifted from the visible band for the $Pt_n^{\bullet+}$ series along with a near-infrared band. The visible and near-infrared absorption bands red shift significantly as the length of the thiophene segment increases. In addition, the spectra of the $Pt_4T_n^{\bullet+}$ oligomers are qualitatively similar to those of the radical cations of thiophene oligomers. For example, Baüerle and co-workers reported that the absorption spectra of the radical cations of a series of alkyl end-capped OThs feature visible bands with maxima at 620, 693, and 725 nm and infrared bands at 940, 1180, and 1250 nm for $n = 3$, 4, and 5, respectively.[70] In a more recent study of non-end-capped OThs, the visible absorption maxima were reported for the radical cations with $n = 2$, 3, 4, 5, and 6 as 425, 545, 648, 730, and 790 nm, respectively.[16] While it is evident that the spectra of the $Pt_4T_n^{\bullet+}$ series are similar to those of the OTh radical cations, the transition energies for the visible and near-infrared bands are red shifted significantly in the $Pt_4T_n^{\bullet+}$ series relative to the position of a thiophene oligomer with a corresponding number of thiophene repeat units. This fact again highlights that, while the positive polaron is concentrated near the thiophene segment, a large fraction of the charge resides on the platinum acetylide units. On the basis of the electrochemical and optical data obtained on the $Pt_4T_n^{\bullet+}$ series, we conclude that the structure illustrated in Scheme 3 provides a reasonable model for the extent of positive polaron delocalization but again the polaron could be slightly longer than depicted.

The optical spectra for the anion radicals, $Pt_4T_n^{\bullet-}$, are significantly different from those of the $Pt_n^{\bullet-}$ ion radicals. This feature also implies that in $Pt_4T_n^{\bullet-}$ the polaron is concentrated near the thiophene segment, although the redox potentials disfavor complete localization there even more than for the radical cations. Reduction potentials for T_1, T_2, and T_3 of −3.22, −2.33, and −1.99 (vs SCE) are 0.7−1.95 V more negative than that of Pt_2. Again the best model seems to be that of Pt centers connected by strong electronic interactions through the T_n groups. Features of the spectra for $Pt_4T_1^{\bullet-}$ and $Pt_4T_2^{\bullet-}$ complexes suggest deocalization of the charge into the phenylene-containing segments of the oligomers. While the spectrum of $Pt_4T_3^{\bullet-}$ exhibits one set of visible and near-infrared bands, the visible absorption of $Pt_4T_1^{\bullet-}$ is split into two distinct bands with maxima at 550 and 615 nm, and the visible absorption of $Pt_4T_2^{\bullet-}$ is a broad, asymmetric band with a pronounced shoulder on the longer wavelength side. The unusual appearance of these optical spectra suggests that the polaron may exist either as a set of equilibrating structures where the charge is localized on either a thiophene or phenylene segment or alternatively as a structure in which the charge is sufficiently delocalized such that it occupies both thiophene and phenylene segments of the chain.

The different behavior of the positive and negative polaron states of the Pt_4T_n series arises due to the difference in spatial distribution of the HOMO and LUMO levels on the oligomer chains. In particular, it is likely that the HOMO level of the Pt_4T_n oligomers is concentrated on the thiophene segment, [—$Pt(P)_2$—C≡C—T_n—C≡C—$Pt(P)_2$—]; the highest filled levels of the phenylene segments, [—$Pt(P)_2$—C≡C—Ph—C≡C—$Pt(P)_2$—], lie several hundred millivolts lower in energy. This explains why the positive polaron is concentrated on the thiophene segment; in essence the polaron is trapped in a thermodynamic well. In contrast, for the shorter Pt_4T_n oligomers, it is likely that the unfilled (LUMO) levels of the thiophene and phenylene segments are very similar in energy. Consequently, even if the negative polaron is spatially concentrated, it has less of a thermodyanic preference to localize on the thiophene segment.

Summary and Conclusions

This study has applied electrochemistry, pulse radiolysis/transient absorption spectroscopy, and density functional theory calculations to study the properties of ion radicals produced by oxidation and reduction of two series of platinum acetylide oligomers, Pt_n and Pt_4T_n. Anodic sweep electrochemistry indicates that the oligomers with $n \geq 2$ platinum centers can be oxidized to produce stable or metastable radical cations at potentials <1.0 V versus SCE. For Pt_3 and Pt_4, the electrochemical data provide evidence that a single platinum acetylide chain can be oxidized two times producing what is believed to be single chains that contain two positive polarons that are concentrated onto separate [$-Pt(P)_2-C\equiv C-Ph-C\equiv C-Pt(P)_2-$] units. Anodic electrochemistry of the Pt_4T_n series indicates that the positive polaron is concentrated on the thiophene segment of the oligomers. Unfortunately, electrochemistry at reductive potentials did not provide useful information regarding the accessible reduced states or stability of the anion radicals.

Pulse radiolysis was used to produce the cation and anion radicals from the Pt_n series, and the dynamics of electron (or hole) attachment and the visible and near-infrared absorption spectra were measured. The attachment rates increase approximately linearly with increasing chain length. All of the oligomer ion radicals exhibit a single, allowed transition in the visible region along with a broad, allowed transition in the near-infrared region. The spectra for the $Pt_n^{\bullet+}$ series converge for $n \geq 3$ whereas those for the $Pt_n^{\bullet-}$ converge for $n \geq 2$. These results suggest that the positive and negative polaron states are spatially concentrated on the platinum acetylide chains. This finding is supported by DFT and TDDFT calculations, which imply that for both the cation and anion radicals the polaron is concentrated in the [$-Pt(P)_2-C\equiv C-Ph-C\equiv C-Pt(P)_2-$] unit. The absorption spectra of the thiophene-containing ion radicals, $Pt_4T_n^{\bullet+}$ and $Pt_4T_n^{\bullet-}$, are distinctly different from those of the phenylene series, which reinforces the electrochemical data in suggesting that the ion radicals are concentrated on the thiophene segment of the oligomers.

While some previous investigations have suggested that platinum acetylide chains can be considered to be "molecular wires",[83] the results of the present study provide strong evidence that in these systems the ion radical states exist as polarons which are spatially concentrated. Charge concentration is apparently driven by geometric distortions which induce self localization of the polaron, although the presence of the platinum centers in the conjugated chain may also contribute to the charge localization. The DFT calculations indicate that coplanar ppp structure is preferred by 2.4 kcal in the cation and 15 kcal in the anion. That strong preference in the anion would be predicted to slow transport of negative charges in these oligomers. Although the results of the present study do not provide a definitive conclusion regarding the "conjugation length" for the polarons, it is fair to say that the polarons are more confined in the platinum acetylide chains than they are in other π-conjugated systems such as poly(thiophene)s or poly(phenylene vinylene)s.

The conclusion that the polaron states are spatially concentrated raises the interesting question: How rapidly does a polaron diffuse along a single platinum acetylide chain? This question is the focus of current pulse radiolysis investigations, and the results will be reported in a forthcoming communication.

Acknowledgment. Work done at the University of Florida was supported by the National Science Foundation (Grant No. CHE-0515066). Work at Brookhaven National Laboratory was supported under Contract DE-AC02-98CH10886 with the U.S. Department of Energy and supported by its Division of Chemical Sciences, Office of Basic Energy Sciences.

Supporting Information Available: Synthetic and characterization details for Pt_4T_n complexes, cyclic voltammograms, plots of electron and hole capture rate constants, additional transient absorption spectra of Pt_3 ion radicals, DFT computed difference charges, and simulated UV−visible absorption spectra for Pt_2 cation and anion radicals (two Schemes, six figures). This material is available free of charge via the Internet at http://pubs.acs.org.

References and Notes

(1) Kohler, A.; Wittmann, H. F.; Friend, R. H.; Khan, M. S.; Lewis, J. *Synth. Met.* **1996**, *77*, 147−150.
(2) McKay, T. J.; Bolger, J. A.; Staromlynska, J.; Davy, J. R. *J. Chem. Phys.* **1998**, *108*, 5537−5541.
(3) Wilson, J. S.; Dhoot, A. S.; Seeley, A.; Khan, M. S.; Kohler, A.; Friend, R. H. *Nature* **2001**, *413*, 828−831.
(4) Cooper, T. M.; Hall, B. C.; Burke, A. R.; Rogers, J. E.; McLean, D. G.; Slagle, J. E.; Fleitz, P. A. *Chem. Mater.* **2004**, *16*, 3215−3217.
(5) Guo, F. Q.; Kim, Y. G.; Reynolds, J. R.; Schanze, K. S. *Chem. Commun.* **2006**, 1887−1889.
(6) Beljonne, D.; Wittmann, H. F.; Kohler, A.; Graham, S.; Younus, M.; Lewis, J.; Raithby, P. R.; Khan, M. S.; Friend, R. H.; Bredas, J. L. *J. Chem. Phys.* **1996**, *105*, 3868−3877.
(7) Chawdhury, N.; Kohler, A.; Friend, R. H.; Younus, M.; Long, N. J.; Raithby, P. R.; Lewis, J. *Macromolecules* **1998**, *31*, 722−727.
(8) Chawdhury, N.; Kohler, A.; Friend, R. H.; Wong, W. Y.; Lewis, J.; Younus, M.; Raithby, P. R.; Corcoran, T. C.; Al-Mandhary, M. R. A.; Khan, M. S. *J. Chem. Phys.* **1999**, *110*, 4963−4970.
(9) Wilson, J. S.; Chawdhury, N.; Al-Mandhary, M. R. A.; Younus, M.; Khan, M. S.; Raithby, P. R.; Kohler, A.; Friend, R. H. *J. Am. Chem. Soc.* **2001**, *123*, 9412−9417.
(10) Kohler, A.; Wilson, J. S.; Friend, R. H.; Al-Suti, M. K.; Khan, M. S.; Gerhard, A.; Bassler, H. *J. Chem. Phys.* **2002**, *116*, 9457−9463.
(11) Liu, Y.; Jiang, S.; Glusac, K.; Powell, D. H.; Anderson, D. F.; Schanze, K. S. *J. Am. Chem. Soc.* **2002**, *124*, 12412−12413.
(12) Wong, W. Y.; Ho, C. L. *Coord. Chem. Rev.* **2006**, *250*, 2627−2690.
(13) Glusac, K.; Kose, M. E.; Jiang, H.; Schanze, K. S. *J. Phys. Chem. B* **2007**, *111*, 929−940.
(14) Warman, J. M.; de Haas, M. P.; Dicker, G.; Grozema, F. C.; Piris, J.; Debije, M. G. *Chem. Mater.* **2004**, *16*, 4600−4609.
(15) Grozema, F. C.; Hoofman, R. J. O. M.; Candeias, L. P.; De Haas, M. P.; Warman, J. M.; Siebbeles, L. D. A. *J. Phys. Chem. A* **2003**, *107*, 5976−5986.
(16) Emmi, S. S.; D'Angelantino, M.; Beggiato, G.; Poggi, G.; geri, A.; Pietropaolo, D.; Zotti, G. *Radiat. Phys. Chem.* **1999**, *54*, 263−269.
(17) Warman, J. M.; Gelinck, G. H.; De Haas, M. P. *J. Phys.: Condens. Matter* **2002**, *14*, 9935−9954.
(18) Burrows, H. D.; Miguel, M. d. G.; Monkman, A. P.; Horsburgh, L. E.; Hamblett, I.; Navaratnam, S. *J. Chem. Phys.* **2000**, *112*, 3082−3089.
(19) Emmi, S. S.; D'Angelantonio, M.; Poggi, G.; Beggiato, G.; Camaioni, N.; Geri, A.; Martelli, A.; Pietropaolo, D.; Zotti, G. *Res. Chem. Intermed.* **1998**, *24*, 1−14.
(20) Hertel, D.; Scherf, U.; Baessler, H. *Adv. Mater.* **1998**, *10*, 1119−1122.
(21) Lee, S. H.; Yasuda, T.; Tsutsui, T. *J. Appl. Phys.* **2004**, *95*, 3825−3827.
(22) Virgili, T.; Lanzani, G.; Cerullo, G.; Gadermaier, C.; Luer, L.; De Silvestri, S.; Bradley, D. D. C. *Trends Opt. Photonics* **2002**, *72*, 374−375.
(23) Hertel, D.; Bassler, H.; Scherf, U.; Horhold, H. H. *J. Chem. Phys.* **1999**, *110*, 9214−9222.
(24) Tseng, H.-E.; Jen, T.-H.; Peng, K.-Y.; Chen, S.-A. *Appl. Phys. Lett.* **2004**, *84*, 1456−1458.
(25) Barth, M.; Guillerez, S.; Bidan, G.; Bras, G.; Lapkowski, M. *Electrochim. Acta* **2000**, *45*, 4409−4417.
(26) Domagala, W.; Lapkowski, M.; Guillerez, S.; Bidan, G. *Electrochim. Acta* **2003**, *48*, 2379−2388.
(27) Frere, P.; Raimundo, J.-M.; Blanchard, P.; Delaunay, J.; Richomme, P.; Sauvajol, J.-L.; Orduna, J.; Garin, J.; Roncali, J. *J. Org. Chem.* **2003**, *68*, 7254−7265.
(28) Ferraris, J. P.; Eissa, M. M.; Brotherston, I. D.; Loveday, D. C.; Moxey, A. A. *J. Electroanal. Chem.* **1998**, *459*, 57.
(29) Jones, N. D.; Wolf, M. O.; Giaquinta, D. M. *Organometallics* **1997**, *16*, 1352.
(30) Graf, D. D.; Mann, K. R. *Inorg. Chem.* **1997**, *36*, 150−157.

(31) Thomas, K. R.; Lin, J. T.; Lin, K. J. *Organometallics* **1999**, *18*, 5285−5291.
(32) John, K. D.; Hopkins, M. D. *Chem. Commun.* **1999**, 589−590.
(33) Zhu, Y.; Wolf, M. O. *J. Am. Chem. Soc.* **2000**, *122*, 10121−10125.
(34) Pappenfus, T. M.; Mann, K. R. *Inorg. Chem.* **2001**, *40*, 6301−6307.
(35) Encinas, S.; Flamigni, L.; Barigelletti, F.; Constable, E. C.; Housecroft, C. E.; Schofield, E. R.; Figgemeier, E.; Fenske, D.; Neuburger, M.; Vos, J. G.; Zehnder, M. *Chem.—Eur. J.* **2002**, *8*, 137−150.
(36) Clot, O.; Akahori, Y.; Moorlag, C.; Leznoff, D. B.; Wolf, M. O.; Batchelor, R. J.; Patrick, B. O.; Ishii, M. *Inorg. Chem.* **2003**, *42*, 2704−2713.
(37) Barbieri, A.; Ventura, B.; Barigelletti, F.; De Nicola, A.; Quesada, M.; Ziessel, R. *Inorg. Chem.* **2004**, *43*, 7359−7368.
(38) Zheng, Q. L.; Bohling, J. C.; Peters, T. B.; Frisch, A. C.; Hampel, F.; Gladysz, J. A. *Chem.—Eur. J.* **2006**, *12*, 6486−6505.
(39) Xu, G. L.; Crutchley, R. J.; DeRosa, M. C.; Pan, Q. J.; Zhang, H. X.; Wang, X. P.; Ren, T. *J. Am. Chem. Soc.* **2005**, *127*, 13354−13363.
(40) Blum, A. S.; Ren, T.; Parish, D. A.; Trammell, S. A.; Moore, M. H.; Kushmerick, J. G.; Xu, G. L.; Deschamps, J. R.; Pollack, S. K.; Shashidhar, R. *J. Am. Chem. Soc.* **2005**, *127*, 10010−10011.
(41) Ren, T.; Xu, G. L. *Comments Inorg. Chem.* **2002**, *23*, 355−380.
(42) Cardlaccia, T. Ph.D. Dissertation, University of Florida, Gainesville, FL, 2005 (http://chem.ufl.edu/∼kschanze/thesis/cardolaccia.pdf).
(43) Wishart, J. F. In *Radiation Chemistry: Present Status and Future Trends*; Jonah, C. D., Rao, B. S. M., Eds.; Elsevier Science: Amsterdam, 2001; Vol. 87, pp 21−35.
(44) Wishart, J. F.; Cook, A. R.; Miller, J. R. *Rev. Sci. Instrum.* **2004**, *75*, 4359−4366.
(45) Miller, J. R.; Penfield, K.; Johnson, M.; Closs, G.; Green, N. In *Photochemistry and Radiation Chemistry: Complementary Methods for the Study of Electron Transfer*; Wishart, J. F., Nocera, D. G., Eds.; American Chemical Scoiety: Washington, DC, 1998; Vol. 254, pp 161−176.
(46) Wang, Y.; Tria, J. J.; Dorfman, L. M. *J. Phys. Chem.* **1979**, *83*, 1946−1951.
(47) Baxendale, J. H.; Beaumond, D.; Rodgers, M. A. J. *Trans. Faraday Soc.* **1970**, *66*, 1996−2003.
(48) Bockrath, B.; Dorfman, L. M. *J. Phys. Chem.* **1973**, *77*, 2618−2622.
(49) Dodelet, J. P.; Freeman, G. R. *Can. J. Chem.* **1975**, *53*, 1263−1274.
(50) Allen, A. O. In *National Standard Reference Data Series; National Bureau of Standards*; US Government Printing Office: Washington, DC, 1976; Vol. 57, p 16.
(51) Frisch, M. J.; Trucks, G. W.; Schlegel, H. B.; Scuseria, G. E.; Robb, M. A.; Cheeseman, J. R.; Montgomery, J. A., Jr.; Vreven, T.; Kudin, K. N.; Burant, J. C.; Millam, J. M.; Iyengar, S. S.; Tomasi, J.; Barone, V.; Mennucci, B.; Cossi, M.; Scalmani, G.; Rega, N.; Petersson, G. A.; Nakatsuji, H.; Hada, M.; Ehara, M.; Toyota, K.; Fukuda, R.; Hasegawa, J.; Ishida, M.; Nakajima, T.; Honda, Y.; Kitao, O.; Nakai, H.; Klene, M.; Li, X.; Knox, J. E.; Hratchian, H. P.; Cross, J. B.; Bakken, V.; Adamo, C.; Jaramillo, J.; Gomperts, R.; Stratmann, R. E.; Yazyev, O.; Austin, A. J.; Cammi, R.; Pomelli, C.; Ochterski, J. W.; Ayala, P. Y.; Morokuma, K.; Voth, G. A.; Salvador, P.; Dannenberg, J. J.; Zakrzewski, V. G.; Dapprich, S.; Daniels, A. D.; Strain, M. C.; Farkas, O.; Malick, D. K.; Rabuck, A. D.; Raghavachari, K.; Foresman, J. B.; Ortiz, J. V.; Cui, Q.; Baboul, A. G.; Clifford, S.; Cioslowski, J.; Stefanov, B. B.; Liu, G.; Liashenko, A.; Piskorz, P.; Komaromi, I.; Martin, R. L.; Fox, D. J.; Keith, T.; Al-Laham, M. A.; Peng, C. Y.; Nanayakkara, A.; Challacombe, M.; Gill, P. M. W.; Johnson, B.; Chen, W.; Wong, M. W.; Gonzalez, C.; Pople, J. A. *Gaussian 03*, revision C.02; Gaussian, Inc.: Wallingford, CT, 2004.
(52) Kondrachova, L.; Paris, K. E.; Sanchez, P. C.; Vega, A. M.; Pyati, R.; Rithner, C. D. *J. Electroanal. Chem.* **2005**, *576*, 287−294.
(53) The poor electrochemical behavior of Pt_5 may arise due to adsorption of the oxidized oligomer on the electrode surface.
(54) Garcia, P.; Pernaut, J. M.; Hapiot, P.; Wintgens, V.; Valat, P.; Garnier, F.; Delabouglise, D. *J. Phys. Chem.* **1993**, *97*, 513−516.
(55) Traytak, S. D. *Chem. Phys. Lett.* **1992**, *197*, 247−254.
(56) Traytak, S. D. *Chem. Phys. Lett.* **1994**, *227*, 180−186.
(57) Funston, A. M.; Silverman, E. E.; Miller, J. R.; Schanze, K. S. *J. Phys. Chem. B* **2004**, *108*, 1544−1555.
(58) Takeda, N.; Asaoka, S.; Miller, J. R. *J. Am. Chem. Soc.* **2006**, *128*, 16073−16082.
(59) Cooper, T. M.; Blaudeau, J. P.; Hall, B. C.; Rogers, J. E.; McLean, D. G.; Liu, Y. L.; Toscano, J. P. *Chem. Phys. Lett.* **2004**, *400*, 239−244.
(60) Glusac, K. D.; Schanze, K. S. *Polym. Prepr.* **2002**, *43*, 87−88.
(61) Van Haare, J. A. E. H.; Havinga, E. E.; Van Dongen, J. L. J.; Janssen, R. A. J.; Cornil, J.; Bredas, J. L. *Chem.—Eur. J.* **1998**, *4*, 1509−1522.
(62) Grozema, F. C.; Candeias, L. P.; Swart, M.; van Duijnen, P. T.; Wildeman, J.; Hadziioanou, G.; Siebbeles, L. D. A.; Warman, J. M. *J. Chem. Phys.* **2002**, *117*, 11366−11378.
(63) Jones, S. C.; Coropceanu, V.; Barlow, S.; Kinnibrugh, T.; Timofeeva, T.; Brédas, J.-L.; Marder, S. R. *J. Am. Chem. Soc.* **2004**, *126*, 11782−11783.
(64) Alberti, A.; Ballarin, B.; Guerra, M.; Macciantelli, D.; Mucci, A.; Parenti, F.; Schenetti, L.; Seeber, R.; Zanardi, C. Phys. *Chem. Chem. Phys.* **2003**, *4*, 1216−1225.
(65) Geskin, V. M.; Dkhissi, A.; Bredas, J. L. *Int. J. Quantum Chem.* **2003**, *91*, 350−354.
(66) Nishinaga, T.; Wakamiya, A.; Yamazaki, D.; Komatsu, K. *J. Am. Chem. Soc.* **2004**, *126*, 3163−3174.
(67) Fichou, D.; Horowitz, G.; Xu, B.; Garnier, F. *Synth. Met.* **1990**, *39*, 243−259.
(68) Guay, J.; Kasai, P.; Diaz, A.; Wu, R.; Tour, J. M.; Dao, L. H. *Chem. Mater.* **1992**, *4*, 1097−1105.
(69) Deussen, M.; Baessler, H. *Chem. Phys.* **1992**, *164*, 247−257.
(70) Bauerle, P.; Segelbacher, U.; Maier, A.; Mehring, M. *J. Am. Chem. Soc.* **1993**, *115*, 10217−10223.
(71) Wintgens, V.; Valat, P.; Garnier, F. *J. Phys. Chem.* **1994**, *98*, 228.
(72) Beljonne, D.; Cornil, J.; Coropceanu, V.; da Silva Filho, D. A.; Geskin, V.; Lazzaroni, R.; Leclere, P.; Bredas, J. L. In *Handbook of Conducting Polymers*, 3rd ed.; Skotheim, T. A., Reynolds, J. R., Eds.; CRC Press: Boca Raton, 2006; pp 1-3−1-46.
(73) Wohlgenannt, M.; Jiang, X. M.; Vardeny, Z. V. *Phys. Rev. B* **2004**, *69*, 241204.
(74) Fratiloiu, S.; Grozerna, F. C.; Koizumi, Y.; Seki, S.; Saeki, A; Tagawa, S.; Dudek, S. P.; Siebbeles, L. D. A. *J. Phys. Chem. B* **2006**, *110*, 5984−5993.
(75) Koizumi, Y.; Seki, S.; Acharya, A.; Saeki, A.; Tagawa, S. *Chem. Lett.* **2004**, *33*, 1290.
(76) Jiao, H. J.; Costuas, K.; Gladysz, J. A.; Halet, J. F.; Guillemot, M.; Toupet, L.; Paul, F.; Lapinte, C. *J. Am. Chem. Soc.* **2003**, *125*, 9511−9522.
(77) Guay, J.; Diaz, A.; Wu, R.; Tour, J. M.; Dao, L. H. *Chem. Mater.* **1992**, *4*, 254.
(78) Bäuerle, P.; Segelbacher, U.; Maier, A.; Mehring, M. *J. Am. Chem. Soc.* **1993**, *115*, 10217.
(79) Furukawa, Y. *J. Phys. Chem.* **1996**, *100*, 15644−15653.
(80) Oberski, J. M.; Greiner, A.; Bassler, H. *Chem. Phys. Lett.* **1991**, *184*, 391−397.
(81) Meerholz, K.; Heinze, J. *Electrochim. Acta* **1996**, *41*, *1839.*
(82) Bauerle, P. *Adv. Mater.* **1992**, *4*, 102−107.
(83) Schull, T. L.; Kushmerick, J. G.; Patterson, C. H.; George, C.; Moore, M. H.; Pollack, S. K.; Shashidhar, R. *J. Am. Chem. Soc.* **2003**, *125*, 3202−3203.